The design of a Space-borne Multispectral Canopy LiDAR to Estimate Global Carbon Stock and Gross Primary Productivity

The design of a Space-borne Multispectral Canopy LiDAR to Estimate Global Carbon Stock and Gross Primary Productivity

Authors: Jim Jack, Emal Rumi, David Henry, Iain Woodhouse, Caroline Nichol and Malcolm Macdonald

Address for correspondence:

Dr Jim Jack
School of Geosciences,
The King's Buildings
The University of Edinburgh,
West Mains Road,
Edinburgh EH9 3JN

Cite As: Jack, J, Rumi, E, Henry, D, Woodhouse, I, Nichol, C & Macdonald, M 2011, 'The design of a Space-borne Multispectral Canopy LiDAR to Estimate Global Carbon Stock and Gross Primary Productivity'. in R Meynart, SP Neeck & H Shimoda (eds), *SENSORS, SYSTEMS, AND NEXT-GENERATION SATELLITES XV*. SPIE-The International Society for Optical Engineering, BELLINGHAM, pp. -, Conference on Sensors, Systems, and Next-Generation Satellites XV, Prague, 19-22 September.

DOI: 10.1117/12.898166

The design of a Space-borne Multispectral Canopy LiDAR to Estimate Global Carbon Stock and Gross Primary Productivity

Jim Jack [a], Emal Rumi *[a], David Henry [b]
[a]School of Geosciences, The University of Edinburgh, West Mains Road, King's Buildings, Crew Building, Edinburgh EH10 5XB, Scotland, UK;
[b]UK Astronomy Technology Centre, Royal Observatory, Blackford Hill, Edinburgh EH9 3HJ

ABSTRACT

Understanding the dynamics of the global carbon cycle is one of the most challenging issues for the scientific community. The ability to measure the magnitude of terrestrial carbon sinks as well as monitoring the short and long term changes is vital for environmental decision making. Forests form a significant part of the terrestrial biosystem and understanding the global carbon cycle, Above Ground Biomass (AGB) and Gross Primary Productivity (GPP) are critical parameters. Current estimates of AGB and GPP are not adequate to support models of the global carbon cycle and more accurate estimates would improve predictions of the future and estimates of the likely behaviour of these sinks. Various vegetation indices have been proposed for the characterisation of forests including canopy height, canopy area, Normalised Difference Vegetation Index (NDVI) and Photochemical Reflectance Index (PRI). Both NDVI and PRI are obtained from a measure of reflectivity at specific wavelengths and have been estimated from passive measurements. The use of multi-spectral LiDAR to measure NDVI and PRI and their vertical distribution within the forest represents a significant improvement over current techniques. This paper describes an approach to the design of an advanced Multi-Spectral Canopy LiDAR, using four wavelengths for measuring the vertical profile of the canopy simultaneously. It is proposed that the instrument be placed on a satellite orbiting the Earth on a sun synchronous polar orbit to provide samples on a rectangular grid at an approximate separation of 1km with a suitable revisit frequency. The systems engineering concept design will be presented.

Keywords: LiDAR, Photochemical Reflectance Index (PRI), Normalized Difference Vegetation (NDVI), Canopy, Above Ground Biomass (AGB), Carbon Stock, Gross Primary Productivity (GPP)

1. INTRODUCTION

Planet Earth's life support system is now under enormous pressure. Human population growth and our contribution to an enhanced greenhouse effect has meant that the future wellbeing of the human race is linked to the physical systems of the Earth that produce food, water, drive climate and replenish natural resources. A key component of this system is the terrestrial biosphere, and especially the world's forests and woodlands. The forests of the Earth contain a significant quantity of carbon and are significant sinks of carbon through photosynthesis. The ability to measure the magnitude of terrestrial carbon sinks as well as monitoring the short and long term changes is vital for environmental decision making. Understanding the amount of atmospheric CO2 being absorbed and released by terrestrial ecosystems is critical for climate change research. This paper describes the concept design of an instrument which provides a measurement capability that can make a significant contribution to the understanding of the global carbon cycle.

A number of parameters are used to understand, model and quantify the behaviour of the terrestrial biosphere in the global carbon cycle, of which the two most important are Above Ground Biomass (AGB) and Gross Primary Production (GPP). AGB is an effective measure of the forest biomass and GPP is an effective measure of the rate of photosynthetic activity. From AGB an estimate of the global carbon stock can be derived. Estimates of forest biomass or AGB have frequently been obtained from a measure of canopy height[1,2]. A species specific algorithm is frequently used to relate canopy height to biomass.

*edrumi@btinternet.com; phone +44-1314478308

The Gross Primary Production (GPP) of vegetation, which is the gross uptake of vegetation through photosynthesis, is defined as the product of the absorbed photosynthetically active radiation (APAR in MJ m^{-2} d^{-1}), which is the absorbed solar radiation between 400-700 nm wavelength, and photosynthetic light-use efficiency (LUE in g C MJ^{-1})). LUE represents the actual efficiency with which a plant can use the absorbed radiation energy to produce biomass[4]. Monteith,[5] first proposed an approach to relate the fraction of photosynthetically active radiation (fPAR) to biomass production that became known as the light use efficiency (LUE) model. The LUE model of gross primary production (GPP in g C m^{-2} d^{-1}) is generally given as:

$$GPP = LUE * APAR$$

Where APAR is generally given as:

$$APAR = \downarrow PAR * fPAR$$

Where ↓PAR is incident photosynthetically active radiation. A wealth of empirical studies[6], large field experiments[7] and theoretical work[7] have demonstrated that the fraction of photosynthetically active radiation (fPAR) is closely related to the normalised difference of the canopy reflectance in the visible and near infrared regions of the electromagnetic spectrum, and termed the Normalized Difference Vegetation Index (NDVI)[6]. Thus if NDVI can be obtained, fPAR may be derived. The NDVI is a simple yet powerful index calculated using reflectance bands centered within the red and NIR regions and calculated as follows:

$$NDVI = \frac{\rho_{NIR} - \rho_{RED}}{\rho_{NIR} + \rho_{RED}}$$

Where ρ denotes reflectance in either the red or near infrared. The direct measurement of LUE, APAR and fPAR is not possible on a global scale and therefore alternative approaches have been investigated to obtain estimates of GPP. Research at Edinburgh University has demonstrated the utility of narrow waveband (or 'hyperspectral') reflectance indices for assessing canopy photosynthetic light use efficiency (LUE) of vegetation[9,10]. The biophysical basis of this approach is well established: when excess light is absorbed by chlorophyll the LUE falls and the relative proportions of a set of accessory pigments, xanthophylls, change and this causes a measurable change in both LUE and the reflectance at 531nm. This change in reflectance at 531nm can be measured with high resolution spectroradiometry and incorporated into a spectral index called 'PRI' (Photochemical Reflectance Index) thus allowing the remote measurement of LUE over whole landscapes. The PRI is one of the few spectral indices which has been shown to be a sensitive indicator of seasonal and diurnal variations in photosynthetic LUE, and its use is therefore particularly attractive in remote measurement of photosynthesis [9,10]. The relationship between LUE and PRI has been demonstrated in a number of studies[11] as shown by Drolet[12], however, these relationships are species dependent and therefore vegetation species is required to select the optimum relationship.

The appropriate reflectance index to detect changes in reflectance requires two narrow wavebands, one centered on 531 nm, which is affected by the de-epoxidation of the xanthophyll pigments, and a reference waveband centered on 570 nm, which remains unaffected by the de-epoxidation reaction [13]. The Photochemical Reflectance Index (PRI) is expressed as PRI:

$$PRI = \frac{\rho_{531} - \rho_{570}}{\rho_{531} + \rho_{570}}$$

Where ρ refers to the narrow-band reflectance centered on the stated wavelength. It is therefore possible to obtain estimates of AGB from estimate of canopy height and GPP from estimates of canopy height, NDVI and PRI. Values for NDVI and PRI may be obtained from measurements of vegetation reflectance at four selected wavelengths 531, 570, 660, and 780 nm.

Obtaining a nearly instantaneous overview of terrestrial AGB, carbon stocks and GPP, has used previous space based sensors. However, Hyde et al. [1] reported that passive multispectral and hyperspectral sensors are of limited use especially in dense forests since they have difficulty penetrating beyond upper canopy layers. Interferometric Synthetic Aperture radar (InSAR) does not seem to reach the desired accuracy unless a forest is structurally homogenous and has relatively low biomass. Multispectral and hyperspectral remote sensing have been used to map structural metrics at moderate resolution and broad scales.

Light Detection And Ranging (LiDAR), on the other hand, is perhaps the most promising remote sensing technology for estimating biomass since it directly measures vertical forest structure by measuring the distance between the sensor and the reflecting surface [2] as well as the reflectance. LiDAR offers 3D information at a high point density and intensity values at a specific wavelength. LiDAR offers the measurements of these indices coupled with canopy height enabling the profile of these indices along the canopy to be estimated. What is missing with the current LiDAR technology is the ability to measure a suite of wavelengths which are sensitive not only to structural elements but also to the spectral reflectance properties of those elements, which are in turn indicative of physiological changes within the leaves [14]. A concept for a satellite mission based on a multi-spectral LiDAR to determine a global AGB and GPP is discussed and is presented in this paper.

2. MISSION CONCEPT

Estimates of NDVI and PRI require measurements of vegetation reflectance at four separate wavelengths. Prior to establishing the mission concept additional requirements must be identified. Changes in forest cover are important and therefore a suitable revisit frequency is required. Revisiting the same location four times each year is considered adequate to detect macroscopic changes. Photosynthetic activity varies during the day, and an optimum time for the observation is between 09.00 and 12.00 local time. The majority of the forest areas of interest are located in the tropics and a polar orbit is chosen. The requirement to meet an observation time suggests a sun-synchronous orbit. Initial instrument mass and power estimates result in an orbit altitude of approximately 400km.

A LiDAR operates by sending a short pulse of radiation to illuminate a footprint and detecting the temporal and intensity profile of the returned scattered radiation. Continuous illumination is not possible. The LiDAR footprint is a compromise between area coverage and spatial resolution. A footprint diameter of 25 to 30m has been recommended by other workers to match the size of a typical large tree[11]. The accurate location of this footprint on the surface of the Earth and the ability to accurately place a revisit footprint over a previous footprint is also important. With the typical space based LiDAR footprint diameter and the limitation on the laser pulse repetition rate, global cover can only be achieved if sparse sampling is adopted.

As the satellite orbits the Earth, a series of LiDAR measurements are made along the ground track directly below the satellite. Subsequent ground tracks are displaced as the orbit is sun-synchronous. These two features are described by the along track spacing of the LiDAR measurements and the across track spacing of the ground tracks. Initial estimates of the satellite orbit characteristics suggest an altitude of approximately 400km, a ground speed of 7.2km/s and a ground track separation of 28km with a 30m diameter footprint. To provide a useful ground cover, cross-track scanning is adopted with a separation between individual footprints of between 1 and 2km. This can be achieved with a repetition rate of nominally 100Hz. This is shown in Figure 1. Thus a swath of sparse samples can be obtained covering the entire Earth in approximately 90 days.

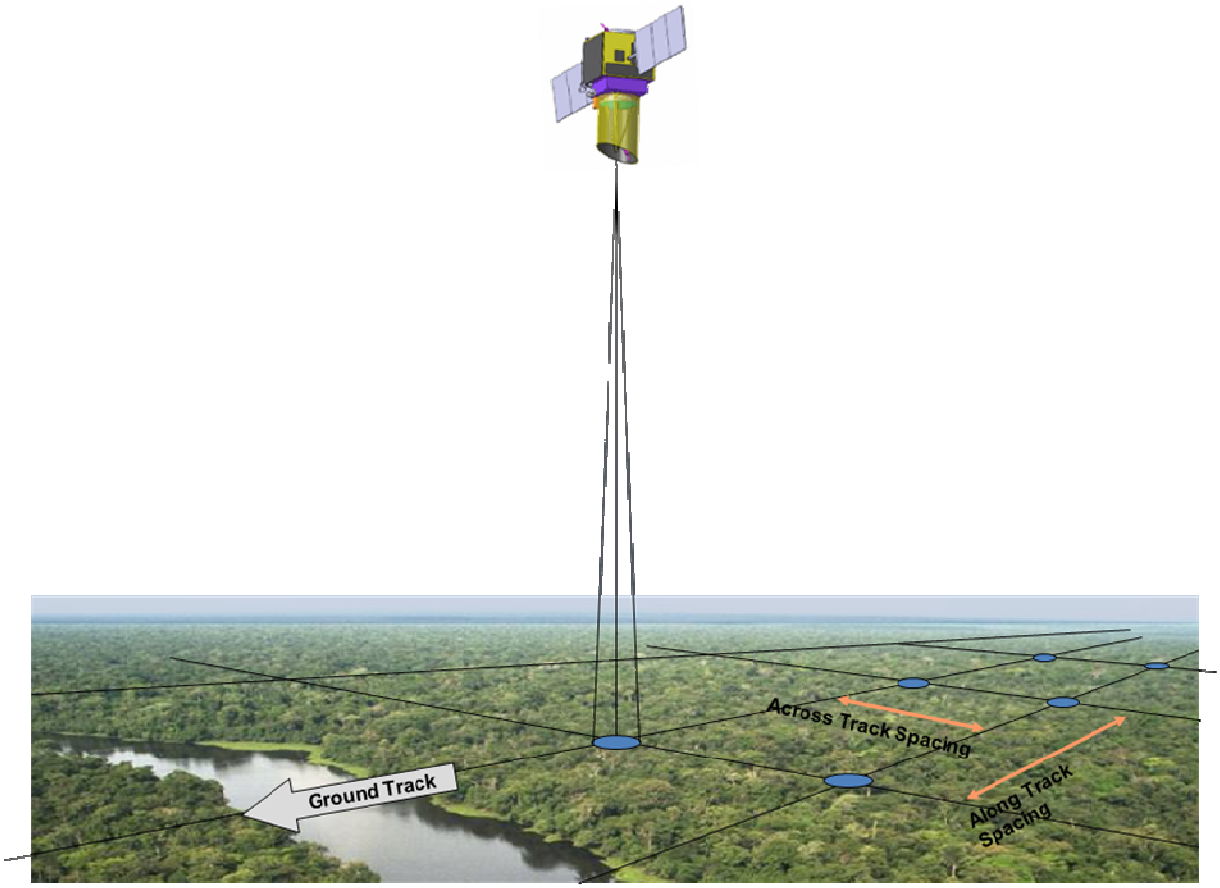

Figure 1. Proposed ground cover with sparse sampling

The basic mission concept is summarized in Table 1. The allometric relationship relating canopy height to AGB suggest the canopy height be measured to a resolution of better than 0.5m. This requirement impacts on the LiDAR pulse duration, the receiver temporal response and the sampling speed and sampling resolution of the digitization.

Table 1. The basic mission concept summary

Parameter	**Value**	**Comment**
Orbit Characteristics	400km altitude, sun-synchronous and descending node between 09.00 and 12.00	Optimum time for measurement of PRI
Revisit Frequency	4 Times per year	To ensure detection of changes
Swath Width	28km	Determined by revisit frequency
LiDAR Footprint Diameter	30m	
Footprint Separation	1km along track and 2km across track	Approximately rectangular pattern
LiDAR Measurement Frequency	100Hz	Limited by constraints on laser PRF.

A range difference of 0.5m results in a time of flight difference of 3.3ns. The signal detected at the receiver will be related to the shape of the emitted laser pulse as modified by the canopy. The determination of range is based on measuring the temporal position of the shape of the emitted and returned signal and this imposes a constraint on the pulse width. A pulse width of 5ns was used in the system model proposed. As a first step, it has been assumed that a sampling rate of approximately ten times the pulse width equivalent frequency is used. Thus the digitization should be carried out at 2GHz.

3. PAYLOAD SYSTEM CONCEPT DESIGN

3.1 The Instrument System Model

The basic systems engineering model is described in the diagram in Figure 2. A tailored LiDAR Equation is derived from the diagram according to a standard approach[12]. Although four separate wavelengths are transmitted simultaneously, the LiDAR Equation is not wavelength specific. When applied to the prediction of the performance of a particular channel, the parameters appropriate to that wavelength must be used.

The transmitter consists of a laser emitting E joules in a pulse length of τ seconds giving E/τ watts instantaneous transmitted power (P_t). The laser pulse is transmitted to the target through the atmosphere which has a transmission of T_1. The distance to the target is R. At the target the reflectance is ρ. The scattered/reflected energy travels back to the receiver and passes through the atmosphere, where the transmission is T_2. The receiver aperture of diameter D collects the scattered energy and passes it through an optical system with transmission T_{RX}. The returned energy reaches a detector with sensitivity S. The angle Φ is the angle between the vertical and the direction of the incident beam nominally zero degrees.

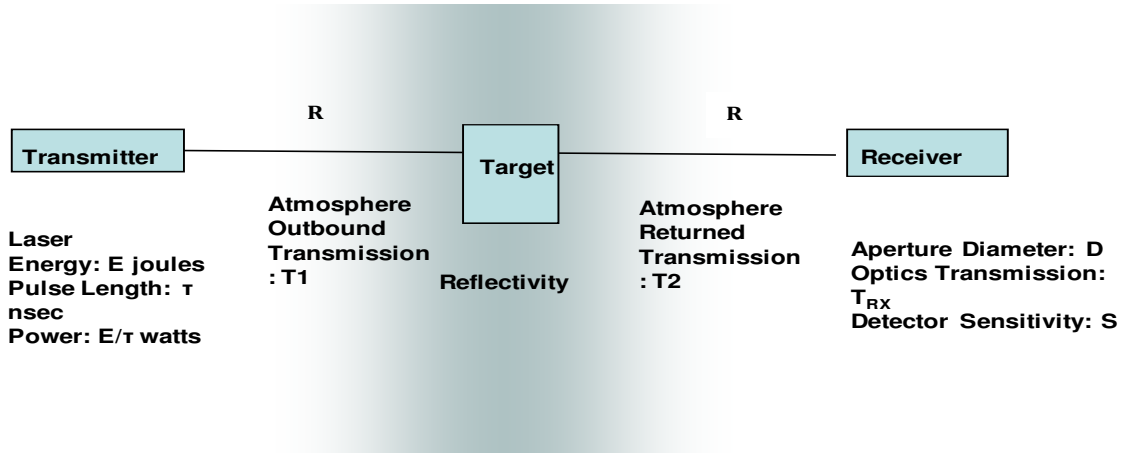

Figure 2. Schematic of LiDAR Model

Using the LiDAR equation, the detected signal can therefore be expressed as[12]:

$$\text{Detected signal} = P_t * T_1 * \rho * \cos\Phi * (1/R^2) * (1/\pi) * T_2 * (\pi * D^2/4) * T_{RX} * S$$

The LiDAR equation can now be used to estimate the laser pulse output energy required to produce adequate signal to noise ratio (SNR) and the instrument characteristics can be established. There are limits on the diameter of the receiver aperture that may be deployed. The current ESA Aeolus Mission has adopted an aperture of 1.5m and this appears a reasonable initial assumption. We may also assume a value for the sensitivity of the receiver based on currently available detector technology. This leaves the atmospheric transmission and the interaction with the vegetation as the remaining variable parameters.

3.2 The interaction with vegetation

The interaction of the beam with the vegetation layer is complex and has been simplified for this model. Several scenarios have been used to obtain an overall system performance. The performance will depend strongly on the density profile of the vegetation. The LiDAR footprint may be considered as intersecting a cylinder of vegetation (ignoring the divergence of the transmit beam over the short distance through the canopy). The altitude resolution of the instrument may be taken as dividing the cylinder into several layers. Within each layer, the reflectivity is measured at the four

wavelengths. However, as the incident pulse travels into the vegetation, the intensity diminishes due to scattering, reflection and absorption. In the worse case no laser energy will reach the forest floor.

The first step is to establish a value for the basic reflectance of the vegetation. Various data bases contain reflectivity values for different examples of vegetation. By considering a range of vegetation spectral signatures from the U.S. Geological Survey (USGS) library, one can see the typical values of reflectance at the specific required wavelengths of a range of vegetation. More than 120 vegetations were studied and Figure 3 shows a selection and Aspen_Leaf-B was selected as a worst case scenario for further system model calculations.

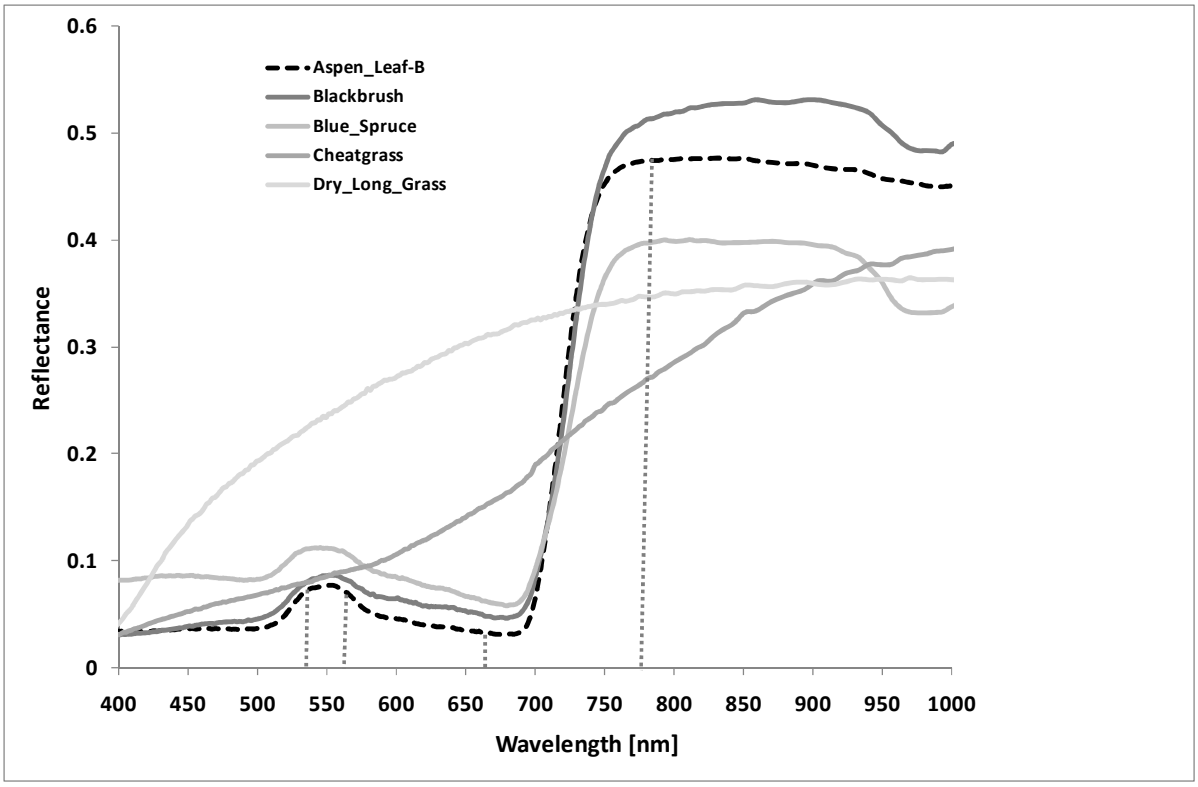

Figure 3. Typical Vegetations Spectral Signatures

Both NDVI and PRI are estimated from a ratio of reflectance values at specific wavelengths, namely 531nm, 570nm for PRI and 660nm and 780nm for NDVI. It may be noted that the value of R(780) is relatively high compared to those at the lower wavelengths and therefore there is a high contrast between R(780) and R(660). However, both R(531) and R(570) are small and the difference between each is also small. This feature requires the instrument sensitivity to be much higher in the green spectral region. Measured (USGS) data has been used to calculate typical values for NDVI and PRI for a range of vegetation types and surfaces. The data suggests it is possible to discriminate between vegetation and non-vegetation. In the system model calculations of the worst case scenario, Aspin_Leaf_B, highlighted with a black dotted line in Figure 3 is used with reflectivities of 0.06761, 0.06128, 0.03259, and 0.475 respectively for 531, 570, 660, and 780nm.

3.3 The Atmosphere

The atmosphere will degrade the transmitted beam and the reflected beam through absorption, scattering and bending. The atmosphere will also add the equivalent of noise through scattering of other sources of illumination into the return beam. The atmosphere will also affect the beam direction causing errors in the knowledge of the ground footprint position. The atmosphere may also modify the shape and divergence of the transmitted and reflected pulse. These effects are different at the four wavelengths. To estimate transmission, a MODTRAN Atmospheric Model for tropical forest scenario was used based on a sensor altitude of 400km. The transmittance values of the atmosphere at the four wavelengths 531, 570, 660, and 780 nm were calculated are 0.5973, 0.6159, 0.6897, and 0.7539 respectively. These

values have been used in the systems modeling. However, it is important to have transmittance values for each LiDAR shot and therefore an on-board means of measuring transmittance is essential.

3.4 Laser Pulse Energy

In the measurement of reflectivity the performance is determined by the trade-off between the laser energy and the SNR of the receiver output. The basic constraints of the geometry, the vegetation reflectance values and the transmission of the atmosphere have been defined. By means of the LiDAR equation, the minimum required laser pulse energy may be calculated that will result in an adequate (SNR) for the mission.

In the basic trade-off between SNR and laser energy, it is assumed that the vegetation comprises a single uniform layer at the same level as the mean canopy height. This is expected to be relevant to the situation of a 100% canopy cover which may exist in some northern hemisphere conifer plantations and also in certain tropical rain forests. A number of additional scenarios must be considered when examining the trade-off between laser energy and SNR. Where the cover is not continuous, part of the incident energy will be reflected and part will pass through the first canopy layer to be reflected from the next level within the canopy. As the canopy cover decreases, the signal from the canopy reduces until the noise is dominant. This can only be compensated for by increasing the laser pulse energy. In the first scenario, it is assumed that the canopy cover is 100% and all the incident laser energy is reflected by the canopy. In the second scenario it is assumed that the canopy cover is 50% and only half of the incident laser energy is reflected by the canopy. In the third scenario, the assumption is made that the canopy intercepts 80% of the footprint and the remaining 20% passes through the canopy and is reflected from the ground. The return from the ground now drives the requirement on the laser energy.

The system model performance was calculated using values previously discussed for reflectance, atmospheric transmittance together with mission characteristics. A value for the receiver sensitivity has been assumed based on the current state-of-the-art receiver modules. The value of SNR was plotted against a range of laser energies for each of the four wavelengths, the case of 100% canopy cover is shown in Figure 4. Based on previous instruments, a value of SNR>20 was assumed to be sufficient as a minimum required. This is shown in Figure 4 as a horizontal dotted line.

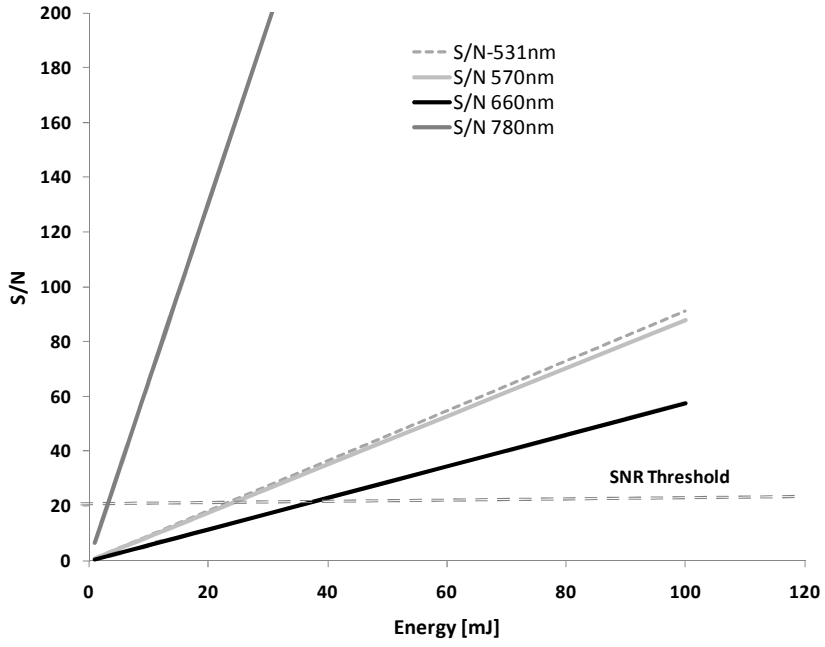

Figure 4. System Model Performance

An analysis for the worst case scenario suggests that the laser output energies required are as shown in Table 3.

Table 3. Laser Energies required for worst case scenario

Wavelength	531nm	570nm	660nm	780nm
Pulse Energy	44mJ	44mJ	70mJ	27mJ

4. INSTRUMENT CONCEPT DESIGN

The instrument concept is based on a four wavelength laser and a large aperture receiver combined with a small angle scanner. The four wavelength laser is a key component and can be derived from a single wavelength laser source by means of frequency conversion. In this way timing coincident emission can be maintained. A solution is shown in Figure 5 where a laser power head is assumed providing a single wavelength input to a frequency conversion unit which uses a combination of techniques to produce the required four wavelengths. These four wavelengths are produced simultaneously and are passed through the scanner to the transmit telescope. The returned radiation is captured by the receiver telescope and passed through the scanner to the beam separation unit where it is separated into the four wavelengths and then conducted to four separate detectors. The use of a common scanner ensures that the optical alignment of the transmitter and the receiver beams is controlled accurately. Receiver and transmitter optics are chosen to provide the required footprint. The instrument configuration is dominated by the optical layout. A large receiver aperture of 1.5m is required to obtain a good SNR in the receiver channels. The scanning mechanism is necessary to achieve cross-track cover. To ensure the alignment between the Transmitter and Receiver paths, the scanner is inserted into both channels and subsequent optics ensures the magnification is appropriate.

Two cameras are provided for high spatial resolution of the area of observation. The instrument is integrated with a space vehicle which provides power, orbit control and data communication and down-link.

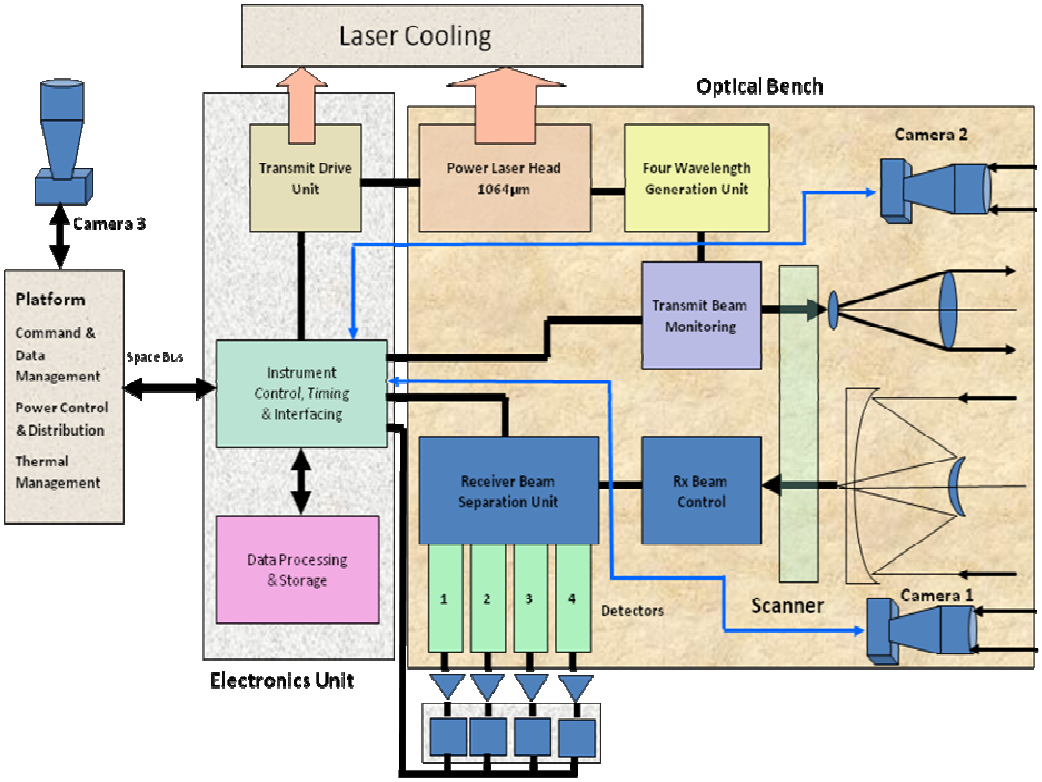

Figure 5. The instrument design concept

4.1 Optics Configuration

Adopting a bi-static configuration means that special attention must be paid to the alignment of the receiver to the transmitted laser beam. In a co-axial configuration the majority of the optical components are either common to both channels or share a common mounting structure. These advantages are reduced for the bi-static configuration. The preferred option will be to build an opto-mechanical system, which is rigid enough to ensure that alignment is maintained following launch and throughout the life of the instrument. Should this not be possible then an active alignment system will be required.

4.2 Transmitter

The laser source produces a pulse comprising four separate wavelengths with the energies shown in Table 3.

A great deal of effort has already been invested in the development of pulsed lasers for space deployment. This has resulted in Nd:YAG becoming a common starting point for the majority of space instruments. The basic output is at a wavelength of 1064nm and techniques have been developed for frequency conversion or wavelength shifting to obtain a variety of different wavelengths from a basic 1064nm source. It is proposed to take advantage of the maturity of Nd:YAG and select this technology for the generation of the initial laser energy. Frequency conversion or wavelength shifting is then employed to obtain the four wavelengths required for the instrument. Various techniques are available for wavelength shifting, including second and third harmonic generation, Optical Parametric Oscillator (OPO) conversion and Raman. However, in the laser power/technical maturity/cost/wavelength trade-space it may be necessary to seek a modification to the ideal requirement.

The first compromise is to select 532nm instead of 531nm as the first PRI wavelength. This wavelength is relatively easy to generate from a 1064nm source using Second Harmonic Generation (SGH) and a conversion efficiency of more than 50% can be achieved. Suitable crystals are readily available. Beta Barium Borate (BBO) offers a wide transmission range and claims of conversion efficiency greater than 70% for SHG have been made by vendors. A more realistic efficiency for SHG frequency conversion might be 60% The efficiency of frequency conversion or wavelength shifting can be as high as 30% for OPO conversion and up to 30% for Raman. It has not been possible to find a solution that generates the four wavelengths from a basic 1064nm source in a single step. Several steps may be required relying on a variety of frequency conversion stages. It is also possible that at each stage a wavelength that is not one of the four may be produced. This may then be re-circulated or dumped. The potential for using these additional wavelengths offers additional functionality. A possible approach to four-wavelength generation is: 1064nm to 532nm via second harmonic generation (SHG), Third harmonic generation (THG) to 355nm via X(3) sum frequency generation, OPO conversion of 355nm to 651 and 780nm signal and idler respectively, and Raman conversion from 532nm to 555nm in potassium gadolinium tungstate (KGW). This would provide output at 355nm, 532nm, 555nm, 651nm and 780nm as well as some residual at 1064nm.

4.3 Receiver

A very high sensitivity low noise receiver is required to detect the small signal return from the LiDAR footprint despite the large receiver aperture. The trade space covering the output pulse energy, beam divergence, receiver field of view and receiver aperture has been examined. The choice has a significant influence on the space craft through the demands on power and thermal management. The current design proposed is for the receiver aperture to be 1.5m diameter and could be based on re-use of the ESA Aeolus transmit telescope. The time of flight for a round-trip laser pulse at an altitude of 400km is 2.67ms. At the maximum laser pulse repetition rate of 100Hz, multiple pulses will not be in transit and each ranging cycle can be completed separately. The choice of detector technology is between photodiodes and Avalanche Photo Diodes. Photodiodes are suitable for low light level detection at high speeds. In these applications, the diodes are operated in photoconductive mode where the detector is reverse biased. The photocurrent is then proportional and linear to the incident light power. The higher reverse bias results in fast response, but results in higher dark generation. The photodiodes are generally responsive from a few nanowatts to a few tens of milliwatts of incident power, thus making them suitable for low noise and wide dynamic range applications. Avalanche photodiodes (APD) provide high sensitivity and better signal to noise ratio by multiplying the photo-generated carriers internally compared to the PN or PIN photodiodes. An optical receiver based on APDs is considered to record the returned laser pulses. Four such receivers are required in the system, one at each wave length of operation. Various techniques for minimizing the noise floor for the detectors will be required and techniques for the extraction of valid returns from noise will also be implemented.

4.4 Scanner

There are a number of options to achieve the required output laser scan pattern and receiver configuration. One option is to design a receiver with a large enough field of view to cover the width of the scan pattern. This requires a telescope with an angular field of view of 30mrad, and a focal plane of ~150mm across. The main drawback for this option is that it requires one detector per scan position and per wavelength, giving a total of 13x4 = 52 separate detectors. A second option is to scan the entire receiver telescope. This requires a telescope with only a small field of view (~100μrad) and a single detector (for each wavelength). It does however require that the receiver telescope be scanned in synchronization with the laser emissions. The large size of the receiver telescope means that scanning the complete telescope is impractical. A third option is to employ completely independent scanning mechanisms in both the receiver and transmitter. The main risk with this approach is that synchronization between the two scanners could be lost, rendering the system unusable. Alignment would also be difficult to maintain. The approach adopted in the concept design is to use a scanning mechanism that is common to both channels. This minimizes the number of detectors used, avoids the need to scan the entire receiver telescope and avoids any issues with synchronization. This is shown schematically in the Figure 6.

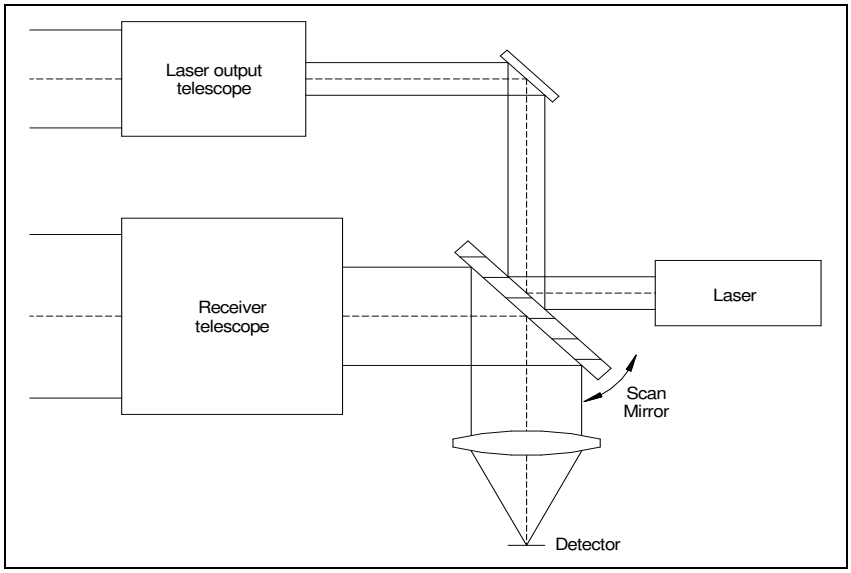

Figure 6. Laser Scanning Schematic

4.5 General and Laser Cameras

The instrument concept includes two cameras to provide information for navigation, attitude accuracy and high resolution imaging of the area around the LiDAR footprint. A General camera provides multi-spectral images on the focal plane each one corresponding to a separate waveband. Images of the forest canopy within the swath are recorded. The camera can therefore be used to measure the homogeneity of the surface vegetation immediately surrounding the LiDAR footprints and provide a context for the measurements. It is also possible that it can be used to determine a species dependent characteristic that can be used to relate canopy height to AGB.

The Laser camera is tuned to be sensitive at the long laser wavelength, 780nm in this case and is designed to detect the illuminated spot on the forest. This camera provides additional measurements of the environmental conditions (e.g. cloud cover) and provides a measurement of the ground location of each laser footprint. Each camera uses 1k x 1k FPA in CMOS technology with separate apertures. Solar background is controlled by suitable filters. The second camera is synchronized to the laser output and integration times are chosen to avoid smearing due to space craft motion. Frame rates are also selected to match the LiDAR repetition rate and space craft ground speed.

5. CONCLUSIONS

This paper has discussed the feasibility of designing and building a Multi-Spectral Canopy LiDAR for deployment in space to make measurements that will improve the estimates of AGB and GPP through measuring canopy height and vegetation reflectivity at four specific wavelengths. An analysis of the science objectives has resulted in the identification of an initial set of mission requirements. These have been used to develop an instrument concept and assess the feasibility of building and launching a suitable instrument. On the basis of this study, it is concluded that a mission is feasible and would result in a significant contribution to the understanding of the global carbon cycle.

AKNOWLEDGEMENT

Professor Rob Lamb and Ian Elder, Selex Galileo Edinburgh, UK. Dr. Cameron Ray, St Andrews University. Dr Caroline Nichol and Dr Iain Woodhouse Edinburgh University.

REFERENCES

[1] Peter Hyde, Ralph Dubayah, Wayne Walker, J. Bryan Blair, Michelle Hofton and Carolyn Hunsaker , "Mapping forest structure for wildlife habitat analysis using multi-sensor (LiDAR, SAR/InSAR, ETM+, Quickbird) synergy," Remote Sensing of Environment, Volume 102, Issues 1-2, 30, 63-73 (2006).

[2] Lefsky, M.A., Cohen, W.B., Parker, G.G., Hardin, D.J., "LiDAR remote sensing for ecosystem studies," BioScience, 51(1), 19-30 (2002).

[3] http://www.nasa.gov/topics/earth/features/forest-height-map.html

[4] Monteith JL,"Climate and Efficiency of Crop Production in Britain," Philosophical Transactions of the Royal Society of London Series B-Biological Sciences 281: 277-294 1977.

[5] Monteith, J. L." Solar radiation and productivity in tropical ecosystems," J Appl Ecol, 9, 747-766 1972.

[6] Tucker C.J., "Red and Photographic Infrared Linear Combinations for Monitoring Vegetation," Remote Sensing of Environment 8: 127-150 1979.

[7] Sellers, P.J., Hall, F.G., Strebel, D.E. and Murphy, R.E.,"An overview of the first international satellite land surface climatology project (ISLSCP) field experiment (FIFE)," J. Geophys. Res., 97(D17), 1934-1837 1992b.

[8] Sellers PJ, Los SO, Tucker CJ, Justice CO, Dazlich DA, Collatz GJ, Randall DA," A Revised Land Surface Parameterization (Sib2) for Atmospheric Gcms .2. The Generation of Global Fields of Terrestrial Biophysical Parameters From Satellite Data," Journal of Climate 9: 706-737 1996.

[9] Nichol C., "Remote sensing of photosynthetic light use efficiency of boreal forest," AgForest Met 101:131-142 2000.

[10] Nichol C.,"Remote Sensing of photosynthetic light use efficiency of Siberian boreal forest," Tellus 54B: 677-687 2002.

[11] Rosette J., North P., Suarez, J. Los S., "Uncertainty within Satellite LiDAR estimations of vegetation and topography," Internation Jouranl of Remote Sensing, 31, 5, 1325-1342 2010.

[12] Measures, R. M., [Laser Remote Sensing, Fundamentals and Applications], Krieger Publishing Company, John Wiley and Sons inc., New York, US, 1984.

[13] Gamon J.A., Serrano L., Surfus J.S.," The Photochemical Reflectance Index: an Optical Indicator of Photosynthetic Radiation Use Efficiency Across Species, Functional Types, and Nutrient Levels," Oecologica 112: 492-501 1997.

[14] Drolet GG, Middleton EM, Huemmrich KF, "Regional mapping of gross light-use efficiency using MODIS spectral indices," Remote Sensing of Environment 112:3064-3078 2008.

[15] Gamon JA, Penuelas J, Field CB.,"A Narrow-Waveband Spectral Index That Tracks Diurnal Changes in Photosynthetic Efficiency,"Remote Sensing of Environment 41: 35-44 1992.

[16] Grace, J., "Can we measure terrestrial photo-synthetic rate from space?," Global Change Biol 13, 1-14 2007.

[17] Lillsand, T.M., Keifer, R. W. and Chipman, J. W., [Remote Sensing and Image Interpretation, Sixth Edition], John Wiley and Sons Inc., US, 2004.